Chapter 2

Novel designs of bell-mouth-converging collector integrated SCPP

As conventional sources of energy are depleting fast, solar energy based devices can only be mass adopted in future if suitable design innovations are conceptualized and investigated to improve its extremely low energy conversion efficiency. In this chapter, a series of new design concepts of solar chimney power plant are proposed and systematically investigated using an experimentally validated numerical model to maximize power generation capacity. A solar chimney consists two important components: a collector and a chimney. In a first, design of a third component called bell-mouth inlet with different orientation is proposed, investigated and optimized along with collector and chimney. Results show that with suitable design changes in collector, chimney and integrating an efficient bell-mouth at the inlet can increase the air velocity and hence turbine output by about 270% compared to the conventional design. Physics behind such high increase in air velocity was also investigated. It is observed that total pressure potential or the static pressure recovery becomes high and uniform along the chimney height in the new design, which is entirely absent in conventional design. An uniform pressure distribution across the chimney height eliminates the recirculation zones thereby enhancing the system capacity to handle higher volume flow rates. Further analysis was conducted by scaling the lab-scale conventional model and proposed optimised design to a 50 kW power plant. Results show that the proposed new system can produce electrical power up-to 1738 kW, which is about 35 times the conventional design can produce. The proposed design has the potential to meet the energy needs of thousands of villages.

2.1 Introduction

Sooner or later, the non-renewable sources of energy such as coal, diesel, petrol etc. would cease to exist due to excessive exploitation by human race. The only alternative would then be to develop efficient technologies to harness renewable sources of energy such as solar energy. Though solar energy is clean and available in abundance, it is not a concentrated source of energy like non-renewable sources of energy. Further, solar energy is available only during the day and other constraints such as cloud cover, intermittent rain etc. put further limitations in efficiently harnessing this energy [21]. These are the reasons that most of the solar based devices have low energy extraction efficiency.

One of the solar based device that holds promising future for power generation is the naturally driven solar chimney power plant (SCPP) (see Fig. 2.1). Probably, this is the only device with which significant hybridisation studies have been done. For example, a solar chimney can be integrated with a wind turbine [110], photovoltaic panel [60], thermal storage [21, 159, 44], desalination plant [6, 80, 105], solar cyclone for harnessing atmosphere air [80], space heating [137], solar cooling using adsorption chiller system [72] etc. Despite such a versatile nature of solar chimney system, its market penetration is quite low for two main reasons.

The first reason is very low efficiency which is below 2% [6]. Energy conversion in SCPP occurs in 4 stages: solar collector first converts the solar radiation into thermal energy, the thermal energy is converted to buoyancy forces which generates kinetic energy, the kinetic energy is transformed into mechanical energy of the wind turbine, the mechanical energy is finally converted into electrical power (P_e) through generator. Owing to inherent losses during various conversion stages, the system efficiency is as low as 0.1% [6]. With such a low

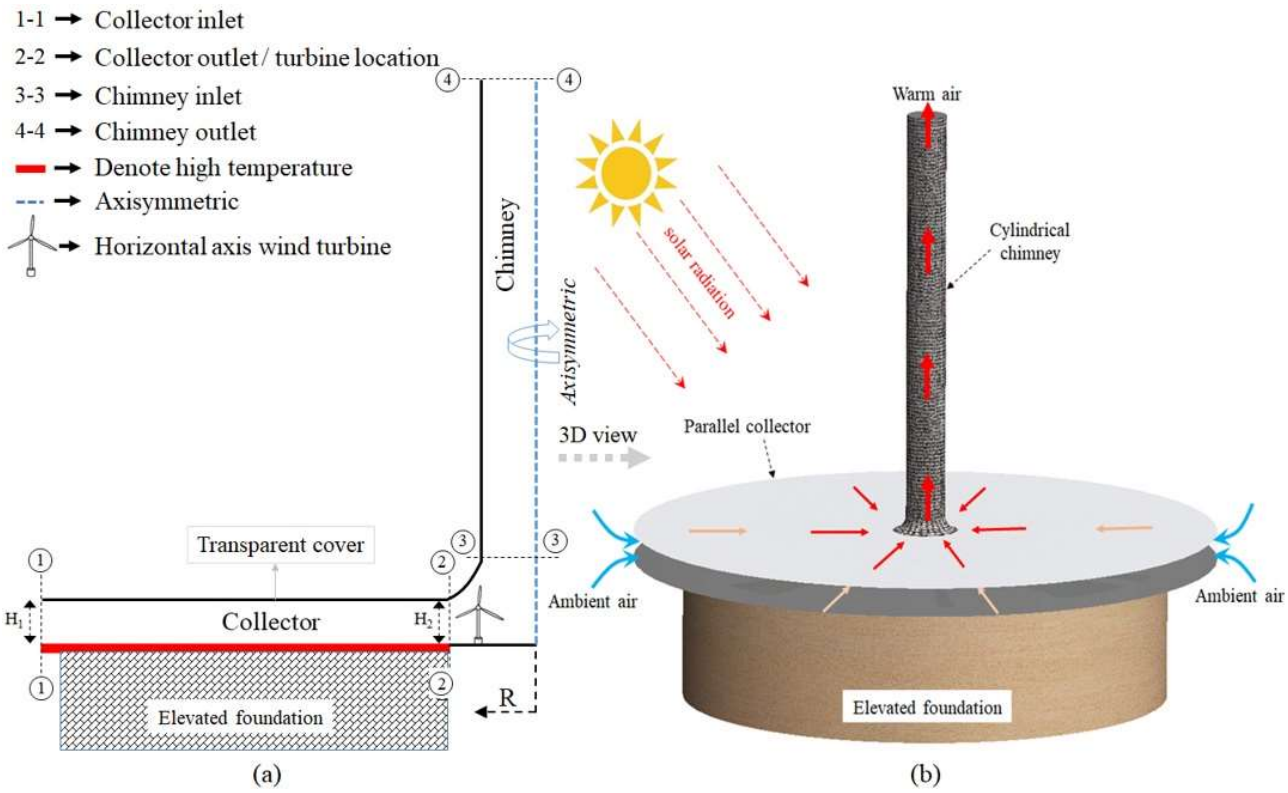

Figure 2.1: Schematic diagram of conventional solar chimney power plant: (a) Two-dimensional axisymmetric model; (b) Three-dimensional view of solar chimney model.

efficiency, hybridising SCPP becomes technologically very challenging. This is the rationale behind previous studies for focusing on increasing the kinetic energy of heated air in SCPP which finally results in higher power generation P_e as P_e is directly proportional to the cube of air velocity i.e. $P_e \propto V^3$ [62, 123].

The second reason for low commercial power generation by SCPP is the cost of such installations. To generate high air velocity, surface area of the collector has to be large which essentially results in high land area requirement. Such installations would be prohibitively costly in cities. If installed in arid or remote region, energy transportation cost becomes high. Hence, owing to the low efficiency and high cost of the SCPP, cost per unit energy produced is currently very high [6]. However, lessons learnt from electric energy production using direct sunlight conversion by photovoltaic (PV) panels is a guiding light to the scientific community. Initially, energy conversion efficiency of PV panel was about 2% and the technology for making such panel was very costly, thus making this PV technology commercially unviable. However, with persistent research by the scientific community and huge money being invested by the various government bodies, efficiency of PV panel has now increased to about 20% [103] with manufacturing cost coming down drastically. Today, the cost per unit energy produced from PV panel has become almost equal to the energy produced from fossil fuels [60, 103]. Thus, taking clue from PV panel history, SCPP can also become economically efficient and viable solution for solar energy harvesting. However, this requires continuous efforts in developing novel designs of SCPP system.

Many efforts have made to improve the efficiency of the conventional SCPP by considering various designs changes specifically in collector duct and solar chimney (see Fig. 2.1), which are two most important component. The circular collector placed horizontally at the ground with a vertical cylindrical chimney installed at the center of the collector. The collector comprises transparent canopy and the ground which constitute the flow passage/channel. The short wavelength radiation passes through the top transparent cover. The canopy of the collector is opaque to the long wavelength radiation and thus, generate greenhouse effect [6]. Due to density difference the ambient air becomes lighter and hence, buoyancy driven flow sustain in the collector flow channel. The wind turbine generally installed at the chimney base driven by the airflow. The ambient air enters from the collector inlet and exit from the chimney outlet. Changing the cylindrical chimney design to a divergent diffuser design significantly enhances air velocity due to static pressure recovery [62, 71, 160, 70, 37, 139]. It is to be mentioned here that design changes in the collector would affect the chimney design, which has been

discussed in this chapter in detailed.

Studies that focussed on designs other than collector duct and solar chimney parameters is scarce in scientific literature. The major objectives of this chapter are three-fold: First, authors propose a new concept of SCPP design that not only synthesise earlier designs but also integrate a bell-shaped inlet at the collector (see Fig. 2.2) that enhances the system performance significantly. Though the concept of adding a bell mouth at the inlet of a natural convection solar air heaters is relatively a new concept introduced by the same authors earlier [137], its performance study in a solar chimney power plant has not yet been investigated in detail. Second, to alleviate the operational deficiencies in the conventional SCPP design due to ambient weather and wind affects. It has been observed that ambient wind severely deteriorate system performance [37]. The proposed innovative design of inlet is expected to minimise the such effects from rain/wind/dust. And third, to exemplify the importance of integrated design concept in SCPP. Authors show in this chapter that optimum design of a component e.g. chimney is not necessarily be the optimum when other component such as collector is modified. Many researchers have investigated designs of collector alone [139, 17, 79, 122, 16] or chimney alone [111, 82, 107]. However, coherent effect of system component designs placed in series from inlet to outlet play a significant role in overall system performance.

2.2 Description of problem

Figure 2.2 shows schematic diagram of a new SCPP incorporating innovative design changes from inlet to outlet sections. When compared to the conventional design (see Fig. 2.1), the new designs cases investigated are: bell-mouth inlet and its orientation (horizontal (Fig. 2.2b), 90° downward bell-mouth (Fig. 2.2c) and 90° upward bell- mouth (figure not shown)); different tapper ratio of collector and divergence ratio of the chimney. A horizontal opening of the collector inlet is expected to be affected by the climatic and environmental wind conditions. A 90° downward bell-mouth, from the design point of view, is opined to be more immune to environmental disturbances. Note that authors have not performed any investigations on water or dust entry or ambient wind effect on the system performances, quantification any which can be part of a different studies. Bell-mouth shape can be changed by changing h and R. Various designs of bell mouth has been investigated for the optimum configuration. Note that such SCPP must be mounted on an elevated foundation to facilitate changes in direction of inlet mouth. These various designs are simulated individually by integrating with convectional design of SCPP and the best design of each configurations were then combined into a single geometry and system performances were investigated. The various design parameters are provided in Table 2.1.

Table 2.1: Design parameters of solar chimney [52].

S. No.	Parameters	Values of parameters
1	Collector inlet, H_1	6 cm (fixed)
2	Collector outlet, H_2	2 - 6 cm
3	Collector radius, R	150 cm
4	Chimney height (fixed)	300 cm
5	Chimney inlet radius, R_{ci}	10 cm (fixed)
6	Chimney outlet to inlet radius ratio, ($CORR = R_o/R_i$)	1, 1.5, 2, 2.5, 3, 3.5, 4, 4.5, 5
7	Bell-mouth design ratio, h/R	0.4 - 1
8	Collector solar irradiance (W/m^2)	850

An experimentally validated numerical model has been used for the analysis. Axisymmetric two-dimensional computational domain was developed and discretized using finite volume method. For better prediction of heat transfer and flow visualization, very fine structured boundary layer mesh was developed in the flow conduit. For the sake of briefness, details of mesh independent study has not shown here. For details about grid independent

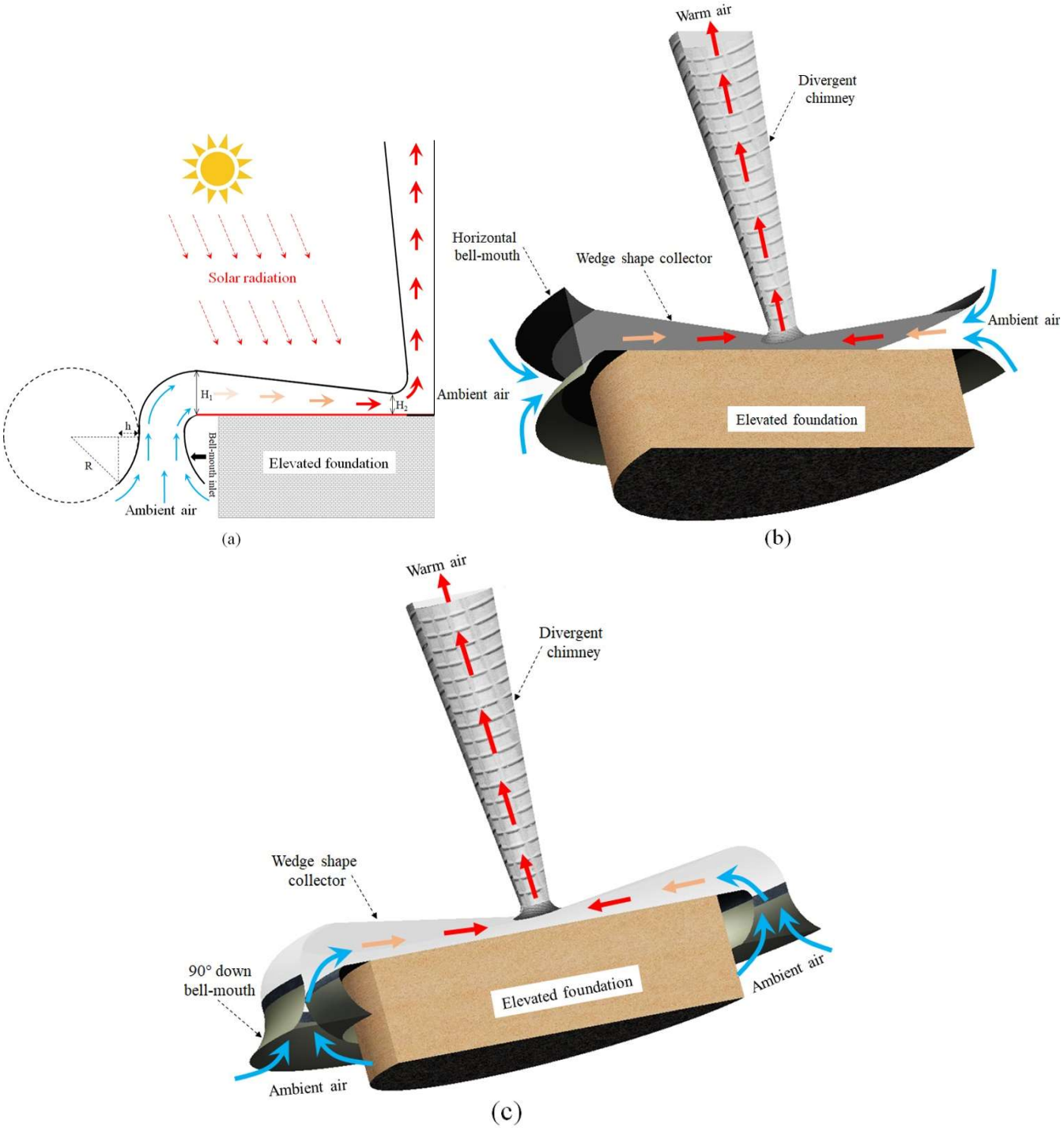

Figure 2.2: (a) Cross-sectional view of the new design of solar chimney power plant put on an elevated position. Notice the design of bell-shaped inlet integrated with the wedge shaped (convergent) collector with divergent chimney. The parametric range bell-mouth design ratio $h/R = 0.4 - 1$, taper ratio $TR = 1.2 - 3$ and $CORR = 1 - 5$; Cross-section of the three-dimensional view of SCPP configuration comprises (b) horizontally placed bell-mouth, and (c) 90° downward bell-mouth inlet- integrated with wedge shape collector-divergent chimney.

test and boundary conditions, interested readers can refer to recent published work by the same authors [139]. The developed model was subjected to necessary boundary conditions to mimic the experimental conditions. The total pressure is zero Pa at the collector inlet which denote standstill environmental condition, whereas the chimney outlet was exposed to atmospheric pressure. The collector was exposed to solar radiation of 850 W/m^2 and top glass assigned to convection heat transfer coefficient 5.7 W/m^2 [150]. Walls of the domain are subjected to no-slip boundary conditions. To simulate practical conditions, the discrete ordinate (DO) radiation model has been considered in the numerical simulations [110, 139].

The flow inside the solar chimney is fully turbulent in nature. The results obtained using standard $k-\varepsilon$ model show more closure values [21, 79, 16] with the experimental data of the literature Ghalamchi et al., 2016 [52]. Below are the basic governing equations considered in the numerical simulations [110, 60, 139].

Continuity equation,

$$\frac{\partial}{\partial x}(\rho u)+\frac{1}{r}\frac{\partial}{\partial r}(r\rho v)=0 \tag{2.1}$$

Momentum equations,

$$\frac{\partial}{\partial x}(\rho uv)+\frac{1}{r}\frac{\partial}{\partial r}(r\rho vv)=-\frac{dp}{dr}+\frac{1}{r}\frac{\partial}{\partial r}\left[(\mu+\mu_t)\,r\frac{\partial v}{\partial r}\right]+\frac{\partial}{\partial x}\left[(\mu+\mu_t)\left(\frac{\partial v}{\partial x}+\frac{\partial u}{\partial r}\right)\right]-2(\mu+\mu_t)\frac{v}{r^2} \tag{2.2}$$

$$\frac{\partial}{\partial x}(\rho uu)+\frac{1}{r}\frac{\partial}{\partial r}(r\rho uv)=-\frac{dp}{dx}+\frac{1}{r}\frac{\partial}{\partial r}\left[(\mu+\mu_t)\,r\left(\frac{\partial u}{\partial x}+\frac{\partial v}{\partial r}\right)\right]+2\frac{\partial}{\partial x}\left[(\mu+\mu_t)\frac{\partial u}{\partial x}\right]+\rho\beta g(T-T_o) \tag{2.3}$$

Energy equation,

$$\frac{\partial}{\partial x}(\rho uT)+\frac{1}{r}\frac{\partial}{\partial r}(r\rho vT)=\frac{1}{r}\frac{\partial}{\partial r}\left[\left(\frac{\mu}{Pr}+\frac{\mu_t}{\sigma_t}\right)r\frac{\partial T}{\partial r}\right]+\frac{\partial}{\partial x}\left[\left(\frac{\mu}{Pr}+\frac{\mu_t}{\sigma_t}\right)\frac{\partial T}{\partial x}\right] \tag{2.4}$$

For the statndard $k-\varepsilon$ model, the equations for turbulent kinetic energy k and dissipation rate of turbulent kinetic energy ε are written as;

$$\frac{1}{r}\frac{\partial}{\partial r}(r\rho vk)+\frac{\partial}{\partial x}(\rho uk)=\frac{1}{r}\frac{\partial}{\partial r}\left[r\left(\mu+\frac{\mu_t}{\sigma_k}\right)\frac{\partial k}{\partial r}\right]+\frac{\partial}{\partial z}\left[\left(\mu+\frac{\mu_t}{\sigma_k}\right)\frac{\partial k}{\partial z}\right]+G_k+\beta g\frac{\mu_t}{Pr_{kt}}\frac{\partial k}{\partial z}-\rho\varepsilon \tag{2.5}$$

$$\frac{1}{r}\frac{\partial}{\partial r}(r\rho u\varepsilon)+\frac{\partial}{\partial x}(\rho u\varepsilon)=\frac{1}{r}\frac{\partial}{\partial r}\left[r\left(\mu+\frac{\mu_t}{\sigma_\varepsilon}\right)\frac{\partial \varepsilon}{\partial r}\right]+\frac{\partial}{\partial x}\left[\left(\mu+\frac{\mu_t}{\sigma_\varepsilon}\right)\frac{\partial \varepsilon}{\partial x}\right]+G_kC_{1\varepsilon}\left(\frac{\varepsilon}{k}\right)-C_{2\varepsilon}\rho\frac{\varepsilon^2}{k} \tag{2.6}$$

where the constants values in the standard k- ε model are taken as $\sigma_k = 1$, $\sigma_\varepsilon = 1.3$, $C_{1\varepsilon} = 1.44$, $C_{2\varepsilon} = 1.92$.

The discretised equations were solved using SIMPLE (semi-implicit method for pressure linked equation) algorithm.

2.3 Experimental validation

To check the authenticity of the numerical model, the data obtained by simulations have been compared with the experimental data of the literature [52]. The model dimensions identical to the experimental setup of Ghalamchi et al., 2016 [52] (see Fig. 2.3(a)) was developed. Dimensions are listed in Table 2.1. Since they reported the results for solar irradiance of 850 W/m^2, the same heat flux was in our model.

Figures 2.3 (b) and (c) shows the velocity and temperature profile, respectively, along the collector radii. It can be seen that model predicts the trend in velocity and temperature variation similar to the experimental data. However, model prediction is consistently higher across the length. About 4-5% higher prediction in temperature from the model is seen near the inlet. Authors discussed here the reasons for higher prediction

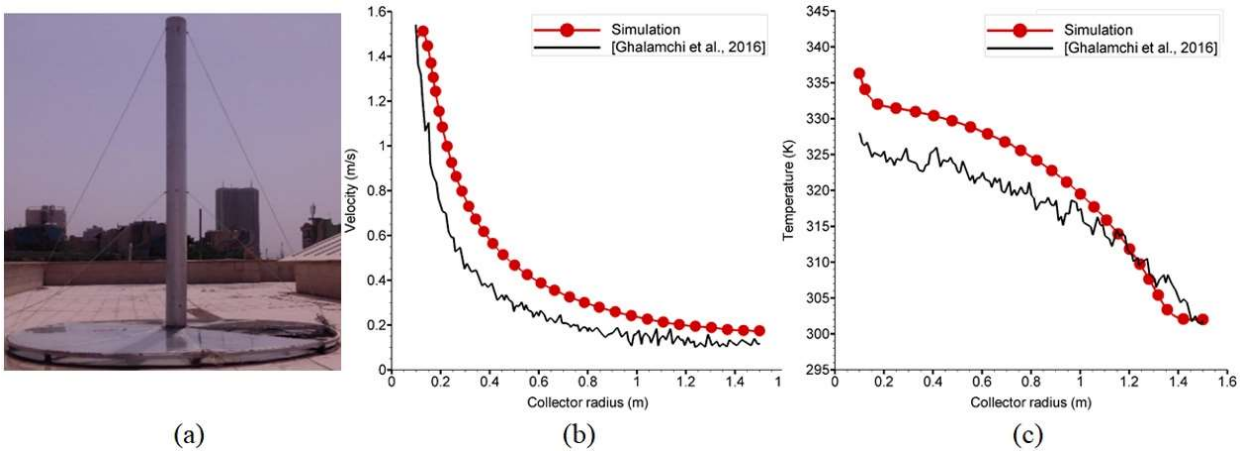

Figure 2.3: (a) Experimental prototype of solar chimney of the literature Ghalamchi et al., 2016 [52]. Comparison of the (b) velocity and (c) temperature profiles using numerical data with the experimental data of the literature Ghalamchi et al., 2016 [52].

[139]. First, we assumed that entire solar irradiance is received by the collector while the actual heat flux received by the collector in the experiments is generally a fraction less due to refraction and reflection from the surfaces and, and second, ambient velocity has some magnitude in experiments contrary to our standstill assumptions. Atmospheric wind contributes to higher heat losses from the system [159, 142]. Third, mounting and fitting in experiments offers resistance to flow while all these losses are absent in the model. Therefore, due to perfect nature of the numerical model, its predictions are a bit higher. Nonetheless, the difference is within the acceptable limit and we can say that the model mimics the experimental conditions.

2.4 Results and discussions

Optimum design of bell-mouth inlet is determined first and then the suitable orientation of the bell-mouth inlet with different bend angle (90° up, 0° horizontal and 90° down) was investigated. The best bell-mouth orientation is further investigated by integrating with wedged shaped collector and divergent chimney.

2.4.1 Bell-mouth orientation and design

It is a fluid mechanics fact that design of inlet effects the losses in the duct Since SCPP represent a typical duct like structure, design of inlet becomes even more important when the primary driving force is the weak buoyancy force [27]. Two extreme angles are considered apart from conventional horizontal design. One is 90°upward and other with 90°facing downward direction as shown in Fig. 2.2(a). The specific dimensions of bell-mouth design would not really matter as along same design and solar insolation is used for all the three conditions.

Figure 2.4 shows the velocity variations along the collector inlet for different orientations of bell-mouth. Following points are noted: (a) In the conventional design, air velocity is non-uniform with higher magnitude is seen near the collector, (b) both 90°upward and downward case shows uniform velocity compared to the conventional case, (c) the velocity profile in the 90° downward bell-mouth attains maximum average flow velocity over larger width opening as compared to the other two cases resulting in higher average velocity. A flatter velocity profile signifies lower hydraulic losses, and (d) about 7.5% increase in velocity was observed with 90° downward bell-mouth compared to the design without bell-mouth integration. Clearly, 90°down configuration seems better choice. Other advantage of down configuration is the problem of water entry during rainy day or dust entry would not be a serious concern. In the next section, best design of bell-mouth shape has been investigated with 90°down configuration.

Next design optimisation was carried out for best bell-mouth ratio h/R (see Fig. 2.2(a)) for the 90° down configuration. It was observed that increasing R and h/R increases the air velocity but velocity decreases beyond a certain h/R ratio. At higher h/R ratio, recirculation zones were observed which increases the overall losses

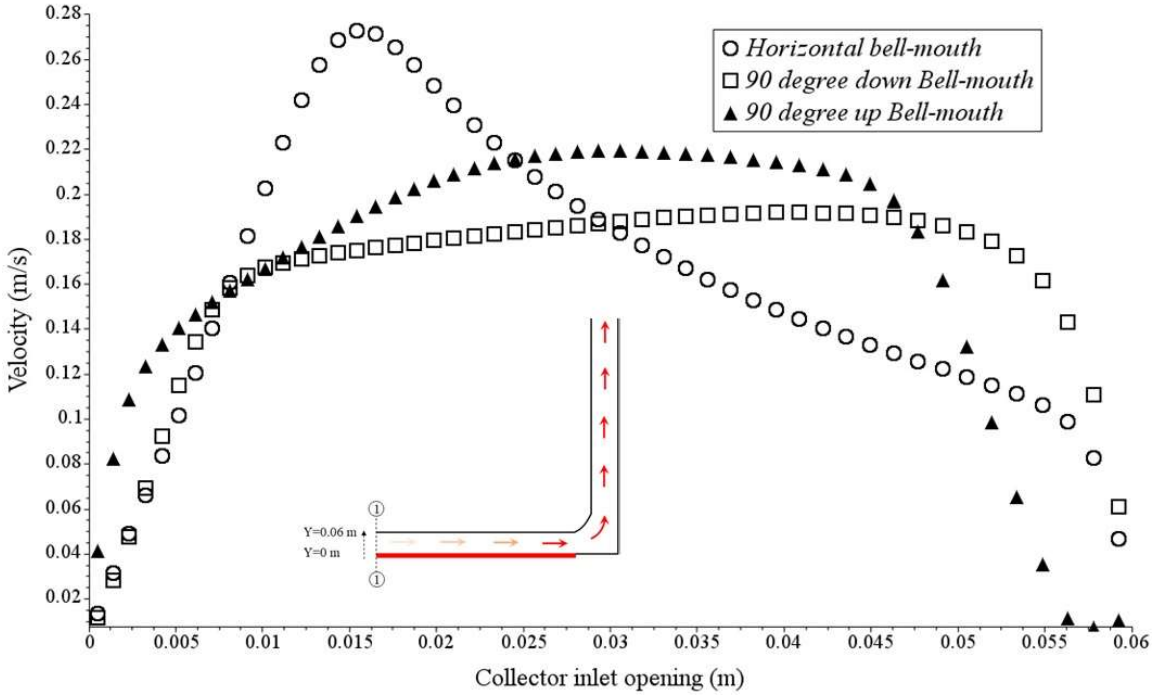

Figure 2.4: Effect on velocity variation at inlet of the collector when integrated with bell-mouth design inlet in conventional SCPP. Bell-mouth with 90° down configuration shows flatter profile across the inlet. Bell-mouth design parameters are: $R = 0.14$ and $h/R = 0.57$. Variation was measured in the marked section 1-1 as shown in inset figure.

in the system. This observation is similar to the previously reported findings [139]. For optimum bell-mouth $R = 0.98$ and $h/R = 0.93$, maximum increase in velocity (by about 7%) was observed. In further simulations and results discussed below, this optimum design of bell mouth has been used.

2.4.2 Effect of 90°down bell-mouth with wedge shaped collector

Collector is the main element in SCPP which receives solar radiation and generate greenhouse effect. The airflow movement inside the collector induce buoyancy forces and the chimney updraft. The collector design is the governing parameter in determining SCPP performance. Collector flow if made wedge shape has its own advantages, but a question arise, whether to construct converging collector channel by either: 1. increasing inlet opening while keeping the collector exit opening constant, or, 2. decreasing the collector exit opening while keeping the collector inlet opening constant. For the same taper ratio *TR,* the later design with decreasing collector exit opening by keeping collector inlet constant show a significant increase in the turbine power output which is about 3 times compared to former technique (discussed later). For more details about the former design, readers can refer the published work by the same authors [139]. Due to drastic increase in the flow velocity at the turbine location by decreasing the collector exit opening is itself a complete study and carried out in this sub-section.

Figure 2.5 shows the effect of wedge shape collector (WSC) on the performance of the solar chimney. Effect of bell mouth inlet design has also shown. Following four points are noted: (i) conventional design show lowest change in velocity along the flow, (ii) flow acceleration along the flow direction increases with the taper ratio and attains high value for TR = 3. Further increase in TR decreased the flow velocity (not shown in figure), (iii) a maximum of 155% increase in velocity was observed in comparison to conventional design just by tapering the collector, (iv) a tapered collector with a bell mouth inlet further enhances the system performance as can be seen in the figure. Its effect can be seen in the heat transfer rate manifested in temperature variation.

Figure 2.6 shows the temperature variation along the collector. The increase in the flow turbulent kinetic energy in the collector enhances the mixing rate as the gap between top transparent cover and the ground gradually reduces. Mixing in the airflow enhances the heat transfer rate and hence increases buoyancy driving potential. Higher temperature variation was recorded for the design associated with the minimum value of $TR = 3$ due to improved heat transfer rate. Further, the WSC with best TR integrated with the best bell-

mouth design at the collector inlet was also investigated. An additional increase of $6-7\%$ in the flow velocity observed due to integration of the bell-mouth design.

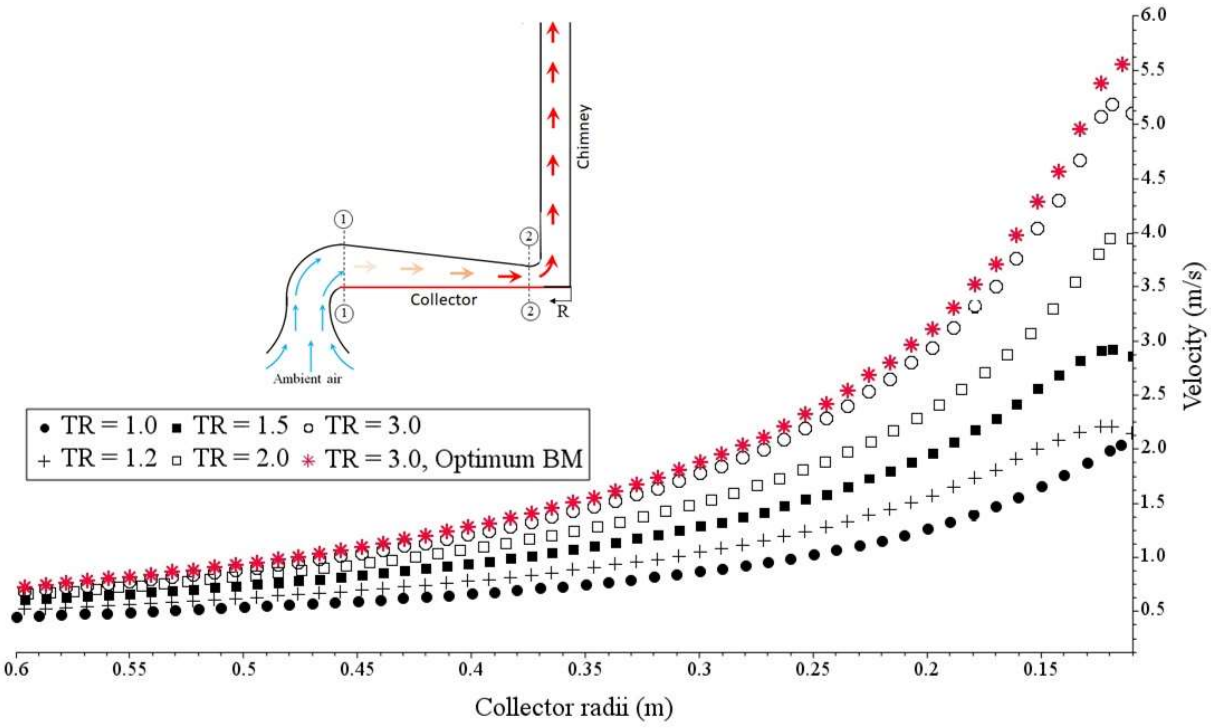

Figure 2.5: Flow velocity variation along collector radius for the taper ratio TR in the range $1-3$ and the best TR i.e. 3 with the best performing bell-mouth design. Measured location 1-1 to 2-2 is shown in inset figure.

The taper flow channel improved the flow velocity at the collector outlet due to recovery in the dynamic pressure $\frac{1}{2}\rho V^2$ on account of reduction in the static pressure. As the TR value decreases, the flow velocity continually improves and becomes maximum for the value $TR = 3$. The corresponding value of pressure falls by 222.5% compared to conventional SCPP design as shown in Fig. 2.7. Further increase in the flow velocity achieved by the integration of bell-mouth design at the wedge shape collector inlet which further decreases the static pressure by 235.5% w.r.t. conventional design. The bell mouth integration creates strong suction pressure which builds additional driving potential for heated air in the collector and chimney.

2.4.3 Effect of wedge shape collector on chimney design

As mentioned earlier, in a fluid conduit consisting of several flow channels connected in parallel, design of each channels would be different when connected in system than when they are operated individually. For example, a parallel solar collector (convection design) connected with a divergent chimney would have a different chimney design for optimum performance than a chimney connected with a convergent or divergent collector. In other words, flow dynamics in the collector would determine the optimum design of chimney. A converging collector can be conceptualized by either enlarging its inlet or converging the exit near the turbine location near chimney inlet. Choice of collector design would depend on the need and application. This section focus on finding out the suitable design of chimney geometric parameters when integrated with the optimum design of collector reported in the previous section.

The power generation of wind turbine in the solar chimney is a strong function of total pressure potential (TPP). The term TPP comprises of two terms: 1. Static pressure recovery (SPR), and 2. Buoyancy. The conversion of dynamic pressure into static pressure denote recovery in the static pressure, which is absent in conventional cylindrical chimney as velocity at the chimney inlet and outlet remains at the same order of magnitude. The term SPR is more pronounced in diffuser/divergent shape chimney which significantly increases the TPP, and hence the flow velocity.

The TPP expression has a functional relationship with the flow velocity at the chimney inlet and outlet and it is expressed as,

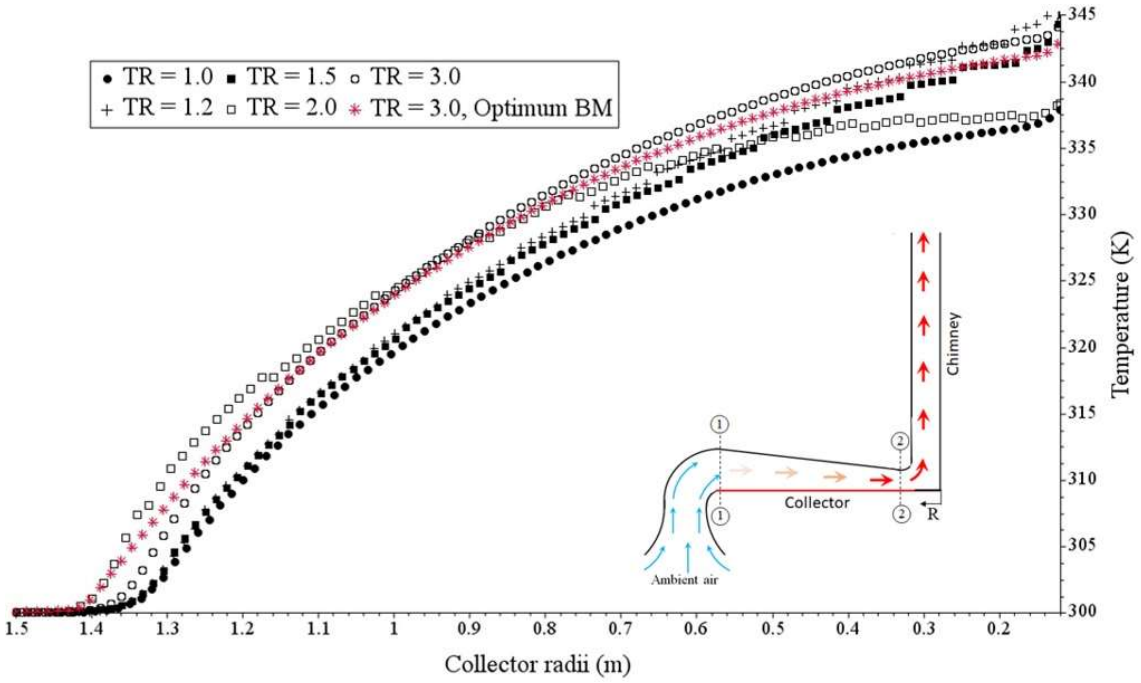

Figure 2.6: Temperature variation along collector radius for the taper ratio TR in the range $1-3$ and the best TR i.e. 3 with the best performing bell-mouth design. Measured location 1-1 to 2-2 is shown in inset figure.

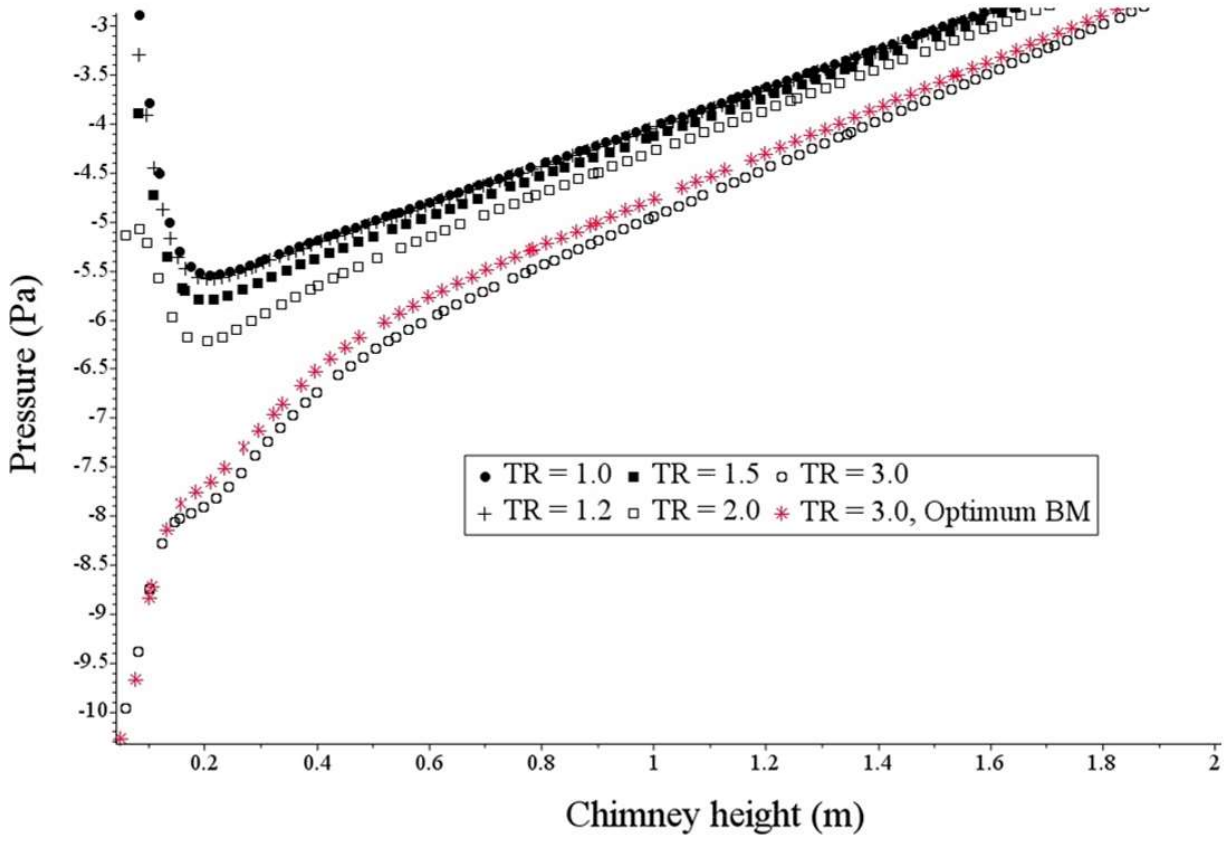

Figure 2.7: Air pressure distribution along chimney height for taper ratio TR in the range $1-3$ and best TR $= 3$ with the optimum bell-mouth.

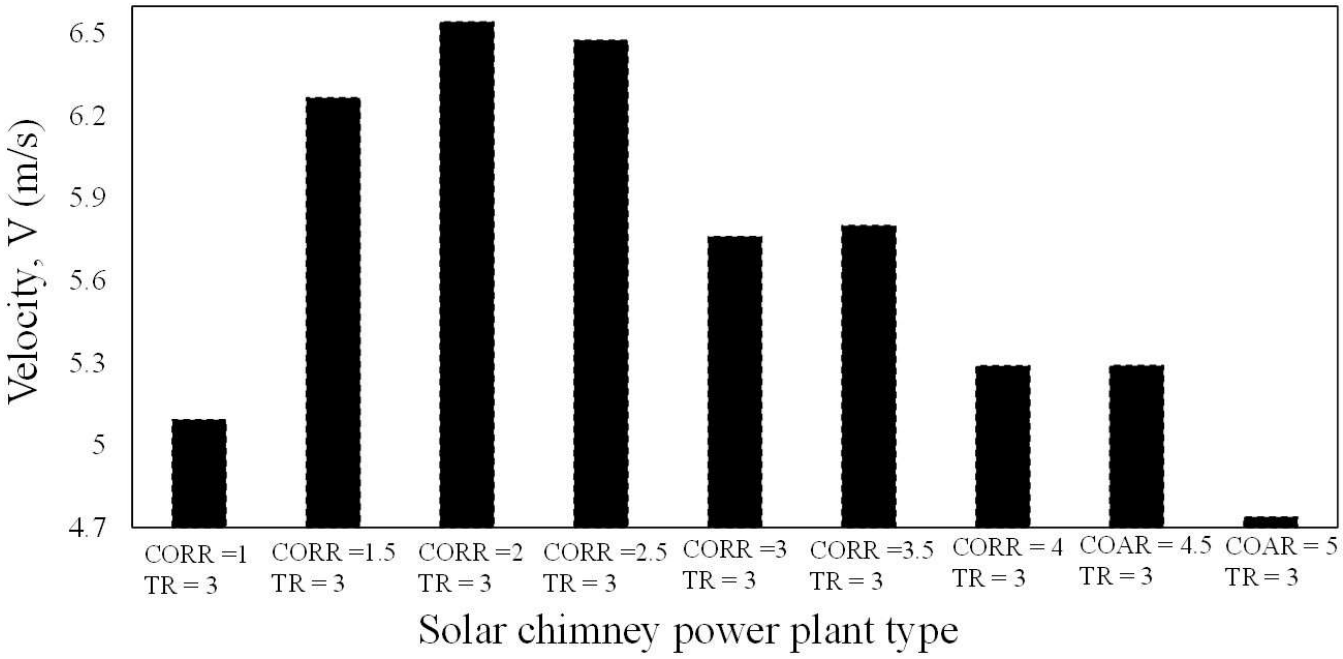

Figure 2.8: Velocity at the collector outlet for the combination: the best wedge shape collector having $TR = 3$ integrated with different divergent chimney for the CORR range $1.5 - 5$.

$$TPP = \frac{1}{2}\rho\left(v_1^2 - v_2^2\right) + \left(\rho_\infty - \rho\right) gH \tag{2.7}$$

where term $\frac{1}{2}\rho\left(v_1^2 - v_2^2\right)$ denote static pressure recovery from the dynamic pressure and $\left(\rho_\infty - \rho\right) gH$ is the flow governed by buoyancy.

Increasing the outlet cross-sectional area of the chimney has a considerable impact on the flow velocity at the collector outlet. Singh et al., 2020 [139] showed that increasing the value of chimney outlet to inlet cross-sectional area (CORR), the flow velocity first increases corresponding to the CORR range $1.5 - 3.5$, but deteriorates the performance at higher CORR. The efficient conversion of dynamic pressure into static pressure at lower CORR aide in enhanced velocity at the chimney inlet. The increase in the flow velocity at the chimney inlet and reduction at the chimney outlet enhanced the total pressure potential (TPP), and hence substantial improvement in the flow velocity. However, the optimum CORR value would be different if the collector design and flow dynamics inside it are different.

Table 2.2: Performance data of various SCPP designs. Note that TR=1 and CORR = 1 represent conventional solar chimney power plant.

TR	CORR	Optimum Bell-mouth	Velocity at collector exit (m/s)	Relative gain in velocity (%)	SPC: $1/2\rho(v_1^2 - v_2^2)$ (N/m^2)	Turbine power (W)
1	1	-	2.02	-	-	0.61
1	3.5	-	4.23	110	12.29	5.62
3	1	-	5.15	155	-	10.15
3	2	-	6.82	238	26.99	23.37
3	2	yes	7.49	270	32.77	31.24

Figure 2.8 shows the flow velocity magnitude for the solar chimney combination i.e. best wedge shape collector $TR = 3$ integrated with the divergent chimney with CORR range $1.5 - 5$. It can be noticed that even with optimum collector design, flow velocity is low with conventional chimney design (CORR = 1). The flow velocity shows increasing trend with increase in CORR value and reached a maximum value of 6.8 m/s for combination $TR = 3$ and $CORR = 2$. This is 240% higher than the conventional solar chimney design. Further increase in the CORR beyond 2 tends to decrease the flow velocity. A marginal fluctuation observed when CORR increased from 3 to 3.5, this happened due to sudden change in flow dynamics with the chimney

flow area which are much pronounced for higher CORR's. Expansion in chimney flow area or sudden expansion amended TPP of the system and hence the slight perturbation was observed. The horizontal axis denote SCPP configuration which varies from left to right, however, each point show a unique SCPP design.

This observation is also observed in local velocity variation (Fig. 2.9). The initial increase is due to improved TPP and deteriorates later due to reverse flow inside the chimney. The decrease in the flow velocity at the turbine location for the higher CORR values occurs due to stall formation at the chimney outlet. For higher CORR's (see Fig. 2.11), the flow moving towards chimney outlet shows the tendency to separate from the chimney wall due to eddies formation (see the enlarged view of showing reverse flow. At the chimney outlet both positive and negative pressure zones exist, the negative pressure region forms recirculation zone which has tendency to mix with the cold ambient air. The flow mixing at the chimney outlet decreases the net flow driving potential. The same phenomenon is observed along the chimney height as shown in Fig. 2.12, where reverse flow along the height near the outlet section for higher CORR's severely deteriorates the overall performance of the SCPP. Significant fluctuations in velocity is seen for higher CORR resulting in adverse pressure gradient formation thereby reducing the system performance significantly.

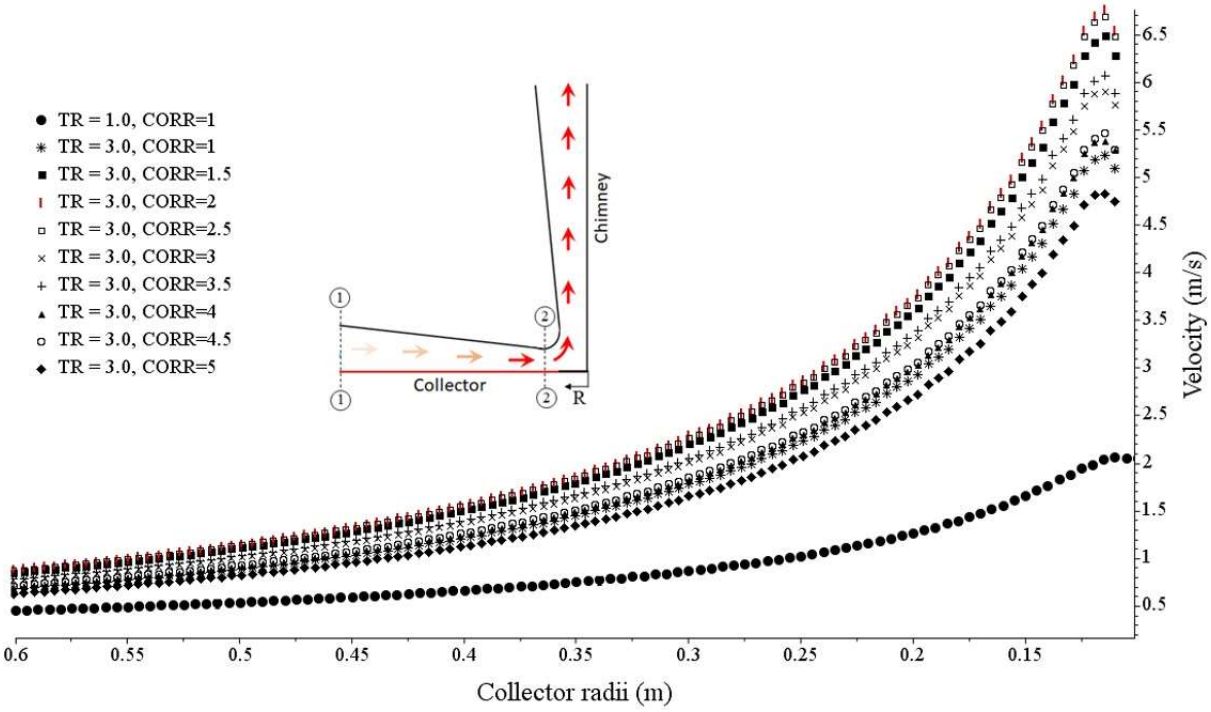

Figure 2.9: Velocity variation along the collector radius of the solar chimney for the combination: the best wedge shape collector having $TR = 3$ integrated with different divergent chimney for the CORR range $1.5 - 5$. Measured location 1-1 to 2-2 is shown in inset figure.

Figure 2.10 shows the air temperature variation along the collector radii for the combination wedge collector and divergent chimney. The air temperature for the CORR range $1.5 - 2.5$ is observed to be lower than the conventional solar chimney design due to increase in the flow velocity. At higher CORR, the temperature profiles higher than the conventional design because of obstruction offered by the eddies formed at the central core of the chimney outlet. The eddies reduces the net flow area for the upcoming flow to exit from the outlet.

An important phenomenon has been observed for the best configuration i.e. $TR = 3$ with $CORR = 2$ is the drop in minimum pressure value to -16.5 Pa, which is 415.6% lower than the conventional design. This considerable decrease in pressure is due to significant increase (by 240%) in the flow velocity. This substantial enhancement in the flow velocity is due to maximum recovery in the static pressure resulting in improvement of total pressure potential of the system.

The best combination of WSC-divergent chimney explored in this section with an aim to further increase the flow velocity by integrating an optimum bell-mouth geometry at the collector inlet, which is reported in next subsection.

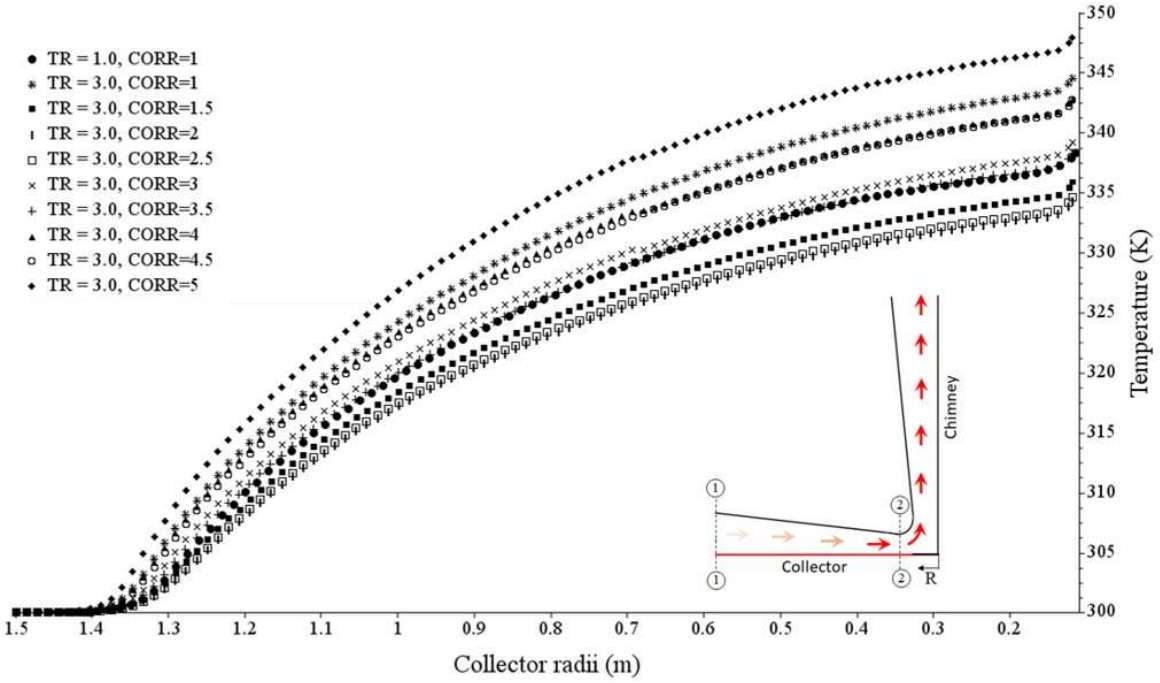

Figure 2.10: Air temperature distribution along the collector radius of the solar chimney for the combination: the best wedge shape collector having $TR = 3$ integrated with different divergent chimney for the CORR range $1.5-5$. Measured location 1-1 to 2-2 is shown in inset figure.

2.4.4 Combined effect of optimum bell-mouth, collector and chimney

In the previous sections, various design configurations of bell shaped inlet, collector and chimney were discussed. Now, the combined effect of all these innovative designs are discussed below and compared with the conventional design.

Figure 2.14 shows the velocity variation along the collector radii for various design configurations. Collector tapper ratio TR = 1 represents conventional parallel design, chimney CORR = 1 represent convectional cylindrical design. It can be noticed from the figure that velocity variation for conventional designs lies at the bottom, lower among all other designs. Case TR = 3 and CORR = 1 corresponds to optimum collector design integrated with the conventional chimney design. An improvement of 155% in the flow velocity was observed. As stated earlier, with conventional collector design (TR = 1), optimum CORR was observed to be 3.5. An increases of about 110% in the flow velocity was achieved. However, when high flow collector design with TR = 3 is integrated, optimum CORR value reduce to 2 i.e. chimney divergence reduced. The combined effect of optimum wedge collector (TR = 3) with optimum chimney design (CORR = 2) show significant improvement with an increase of 240% in the flow velocity. Further enhancement in the flow velocity was achieved with the integration of bell-mouth opening at the inlet of the collector with $TR = 3$ with optimum chimney design ($CORR = 2$) . A substantial 270% increase in velocity was observed, which is the overall best performing configuration of solar chimney plant among all the considered cases. The performance improvement for each case is shown in Table 2.2.

Now let us understand the physics behind significant increase in velocity as discussed above (Fig. 2.14) when the system is integrated with efficient designs of collector inlet, collector and chimney. To illustrate the point, three cases have been taken to relate with the total pressure potential and hence, static pressure gain at the expense of dynamic pressure (see Fig. 2.15). With conventional collector (TR = 1) is integrated with wider chimney at the top (CORR = 3.5), substantial gain in static pressure is observed only towards the chimney exit. In contrast, this gain is lowest at the chimney bottom where turbine is mounted. For the case of optimised design of collector (TR = 3) and chimney (CORR = 2), static pressure recovery at the bottom improves significantly. For example, at chimney height of 0.2 m from the ground, about 2.43 times increase in static pressure is observed compared to the conventional case. Interestingly, with the addition of bell mouth at the inlet, this gain increased by about 3 times at the bottom with near uniform static pressure recovery across the chimney height. The substantial increase in static pressure increases the total pressure potential

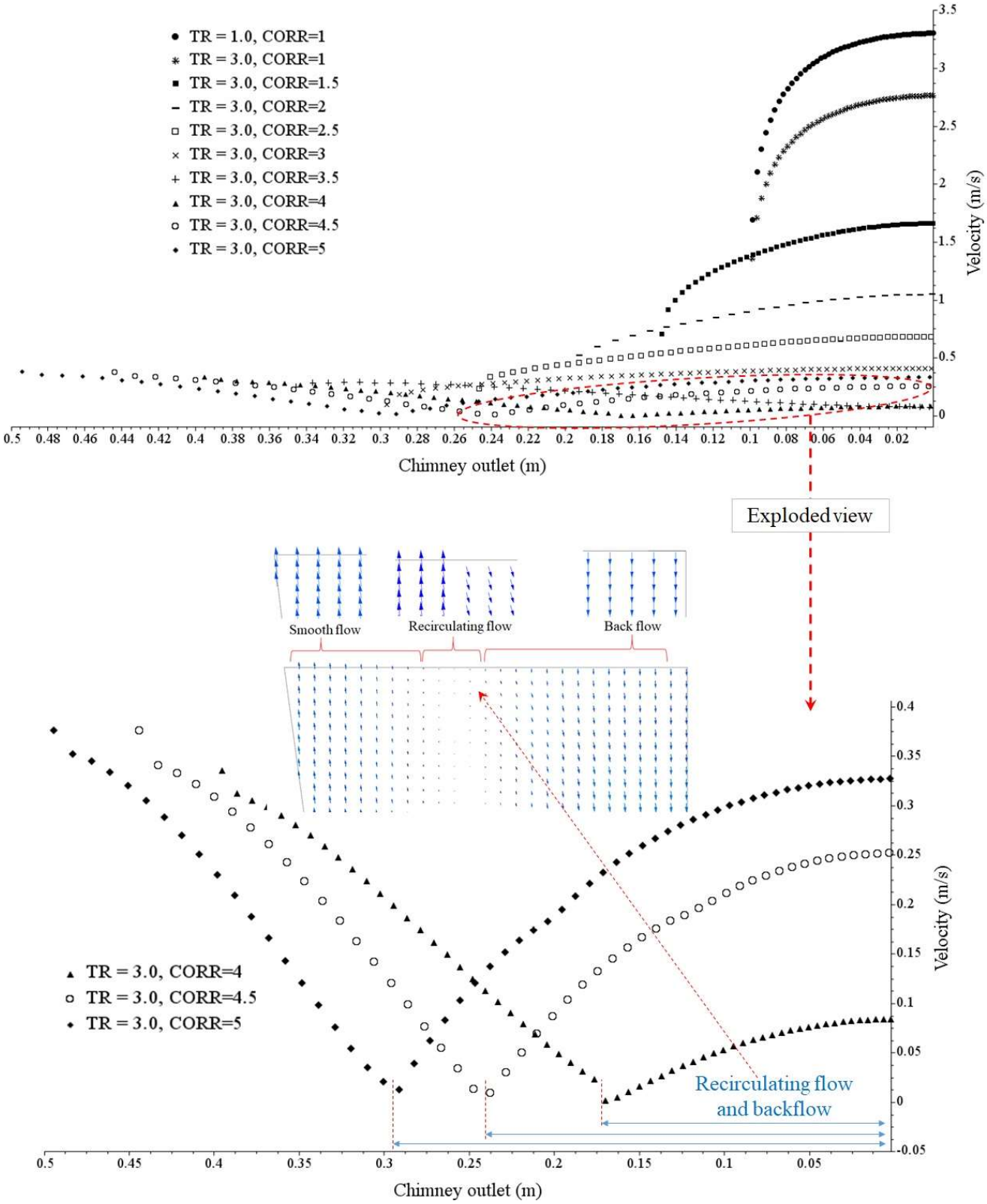

Figure 2.11: Velocity variation at the chimney outlet of the solar chimney for the combination: the best wedge shape collector having $TR = 3$ integrated with different divergent chimney for the CORR range $1.5 - 5$. The enlarged value of higher CORR values 4, 4.5, and 5 with velocity contours shows how velocity fluctuates across the exit length due to recirculation zone formation.

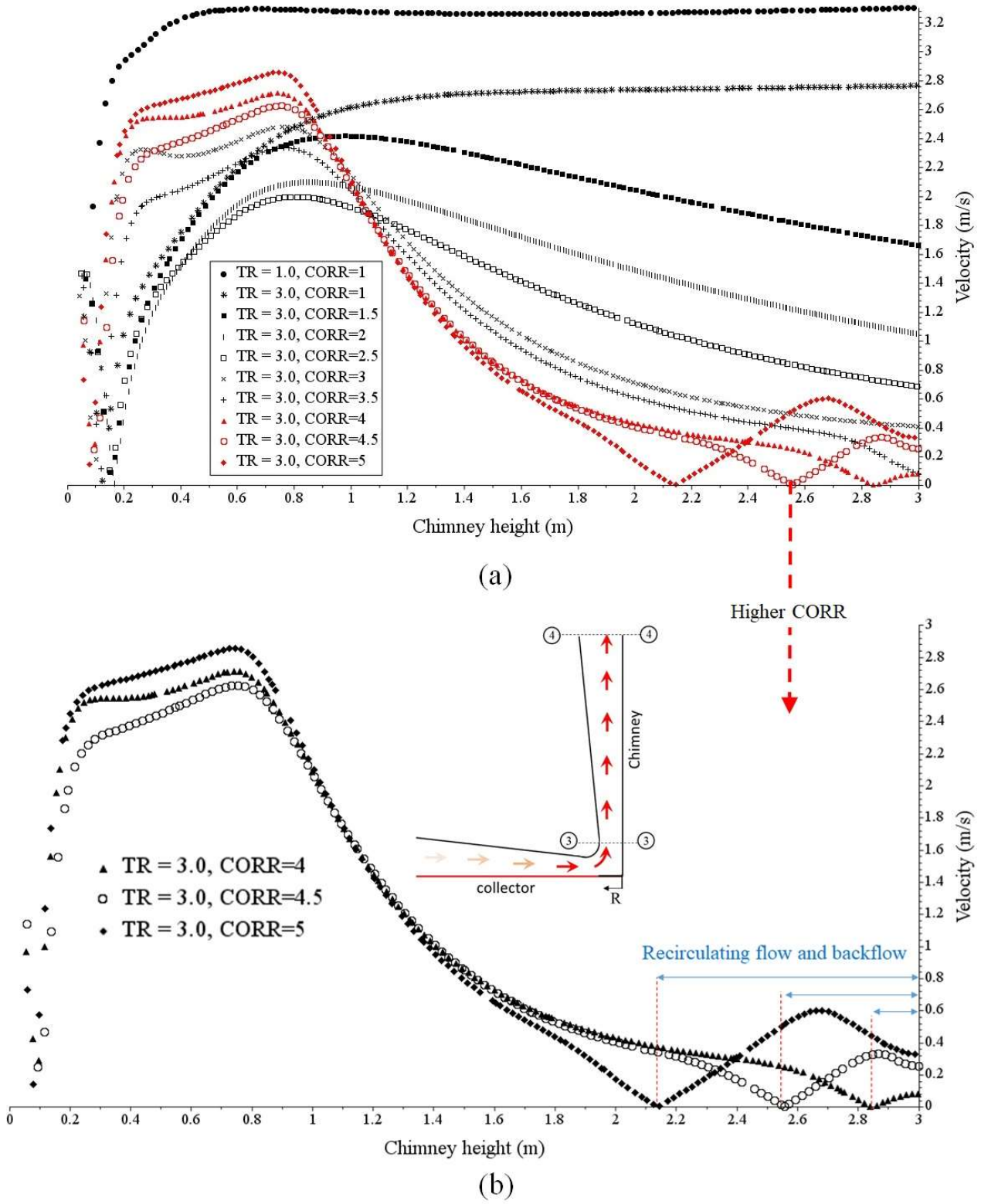

Figure 2.12: (a) Velocity distribution along chimney height from section 3-3 to 4-4 (inset shown) for the combination: the best wedge shape collector having $TR = 3$ integrated with different divergent chimney for the CORR range $1.5 - 5$, (b) Enlarged view of velocity variation at higher CORR clearly depicting significant fluctuations in velocity magnitude due to adverse pressure gradient developed along the chimney height.

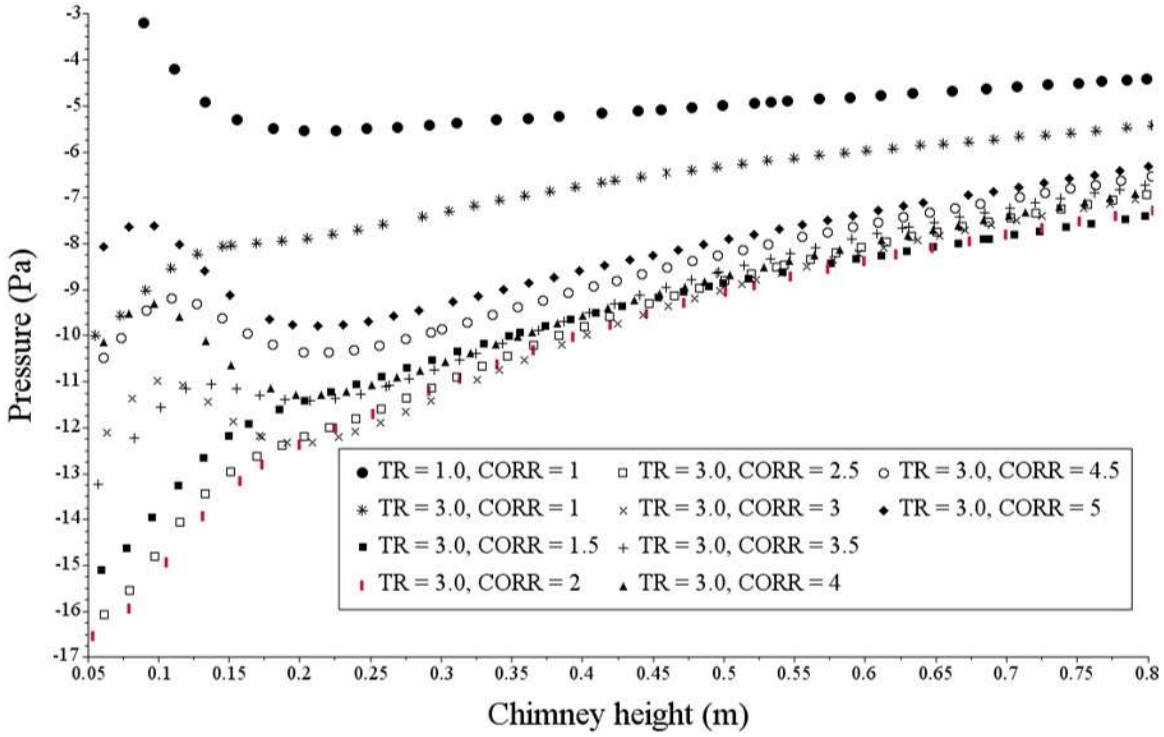

Figure 2.13: Air pressure distribution along chimney height for the system with optimum wedge shape collector ($TR = 3$) integrated with different divergent chimney having CORR range $1.5 - 5$. Note that $TR = 3$ an $CORR = 2$ exhibits higher pressure difference thereby enhancing driving potential.

significantly. Contours of static pressure recovery (SPR) $\rho\left(v_1^2 - v_2^2\right)/2$ are shown in figure 2.16 for the cases discussed above along with the conventional design. It can be noticed that conventional design (Fig. 2.16a) shows negligible pressure recovery due to uniform velocity inside the chimney while the optimum design (bell-mouth inlet integrated with tapered collector and divergent chimney) shows significantly higher static pressure recovery and thus, enhancing the system capability to handle higher volume flow rates of air.

2.4.5 Effect of large-scale model

Results discussed in previous sections are for a lab-scale model. SCPP known for its large physical dimensions and lower electrical power output. To estimate the power producing potential of the new designs, the conventional model of Fig. 2.1 and optimised design of Fig. 2.2(c) are scaled by 81.34 times to bring the new collector dimensions of 50 kW pilot plant installed in Manzanares [58]. The collector area is kept identical in both the designs so that energy input remains the same. The new design has optimum bell-mouth, $TR = 3$, and $CORR = 2$. Results show that velocity in conventional design was 13.27 m/s where it significantly increased to 43.31 in the proposed design. In terms of electrical power output, it is 287 kW and 9981.5 kW in conventional and proposed system, which is about 35 times. First time such significant increase in power output has been reported in the literature. The proposed new designs are simple and easy to construct. If multiple of such designs are installed in the regions which are good in sunshine, it can meet electrical power needs of almost thousands of villages.

2.5 Conclusion

In this chapter, innovative designs are proposed and analysed for maximising the power generation capacity of conventional solar chimney power plant that suffers from extremely low energy conversion efficiency. Apart from design changes in collector duct and chimney, for the first time, a third component in terms of bell-mouth inlet was conceptualised and integrated in the power plant. It was observed that customary horizontal inlet performs poorly. The optimised bell-mouth design oriented in downward direction boosts overall performance of the solar plant by about 33% compared to the conventional designs. However, such design of bell-mouth and its

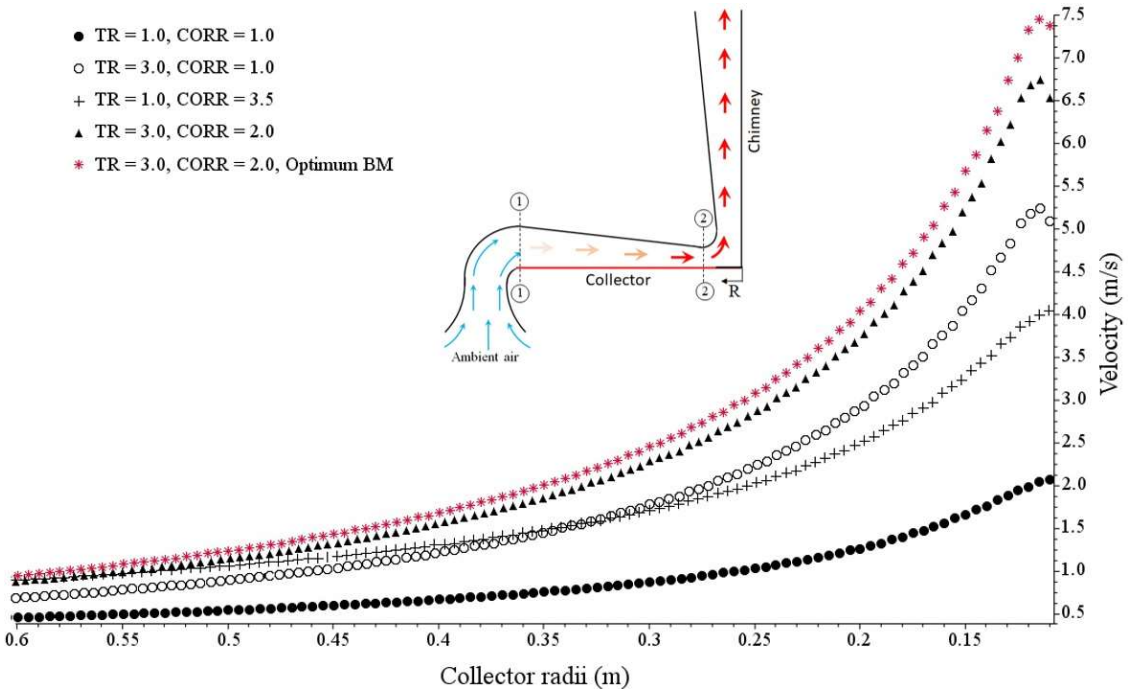

Figure 2.14: Velocity variation along the collector radii for the best solar chimney design for each discussed cases: 1. Only wedge shape collector, 2. Only divergent chimney, 3. Wedge shape collector integrated with divergent chimney, and 4. Bell-mouth opening at the inlet of wedge shape collector integrated with divergent chimney. Measured location 1-1 to 2-2 is shown in inset figure.

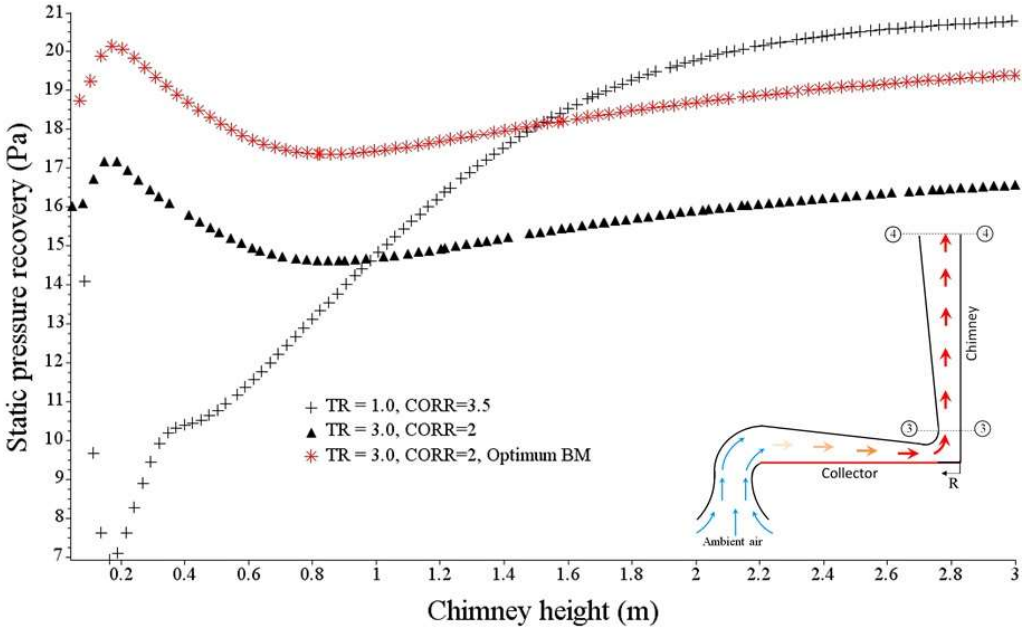

Figure 2.15: Static pressure recovery variation along the chimney height for the best configuration from each case: 1. Only divergent chimney, 2. Wedge shape collector integrated with divergent chimney, and 3. Bell-mouth opening at the inlet of wedge shape collector integrated with divergent chimney. Measured location 3-3 to 4-4 is shown in inset figure. Note that the higher static pressure recovery along the chimney height is observed with the integration of bell-mouth at the inlet.

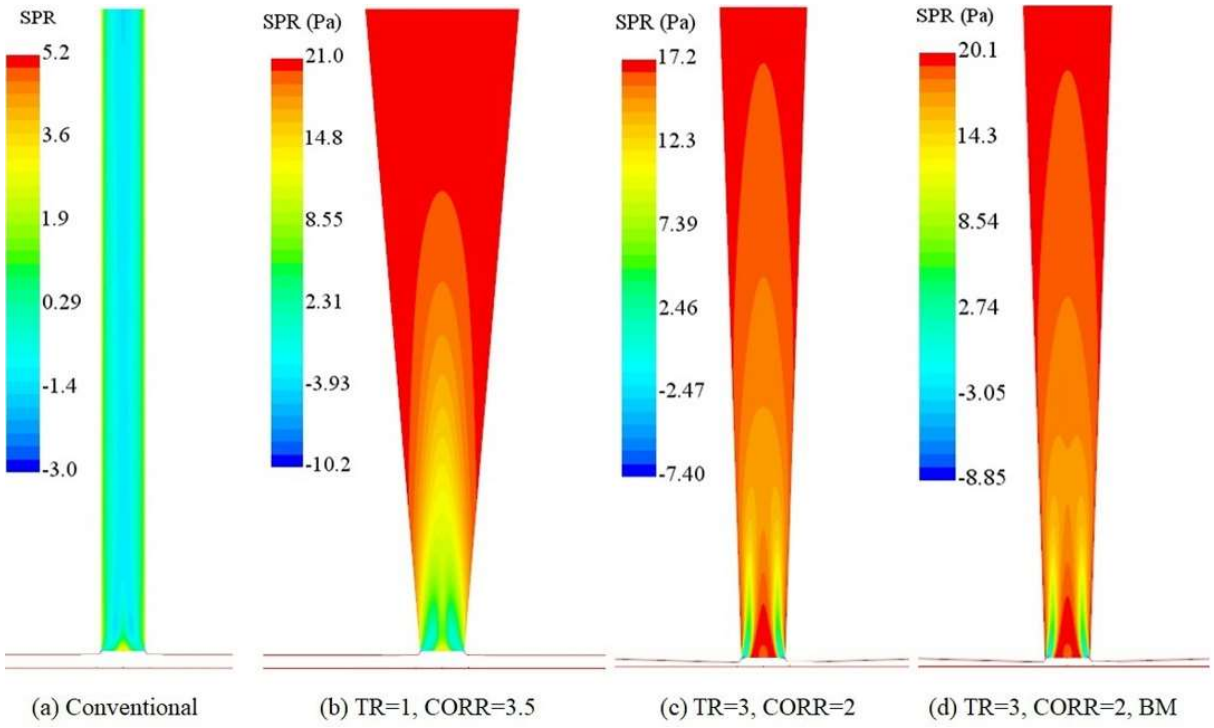

Figure 2.16: Contour plot of static pressure recovery have shown to compare the best solar chimney design comprised of best tapper collector, divergent chimney, and bell-mouth shaped collector inlet i.e. $TR = 3$, $CORR = 2$ and optimum BM, respectively, to compare best design results with the conventional solar chimney design.

integration would require the system to be placed on an elevated foundation. The proposed design of bell-mouth is expected to reduce the ambient wind effect, dust and water entry problem, though no such analysis has been performed in this chapter. Results show that design adaption in collector and chimney is indispensable to take the advantage of bell-mouth inlet design. Numerous designs of tapered collector and divergent chimney was investigated along with the optimised bell-mouth design. It was observed that when chimney alone is optimized, increase in velocity was about 110% with conventional collector, and when both collector and chimney are optimized, increase in velocity was 240% . However, when the optimised bell-mouth is integrated with the optimised collector and chimney, a significant increase in velocity by 270% was observed. The physics behind this enhanced velocity was further investigated. It was observed that bell-mouth integration makes the static pressure recovery uniform along the chimney height thereby enhancing the chimney's capacity to handle higher volume flow rates without getting susceptible to recirculation zones formation at the outlet. Though these investigations are based on lab-scale model, the physics behind the enhanced system performance is expected to remain the same in large-scale model. Further investigation were carried out in 287 kW conventional power plant by uniformly scaling the optimised lab-scale model. The collector area that receives the suns' energy was kept the same in both the cases. Results thus obtained are highly encouraging. The scaled model with bell-mouth and optimised collector-chimney design produced 9981.5 kW of electrical power, which is about 35 times the conventional design. First time such significant increase in power output has been reported in the literature. The proposed new designs are simple and easy to construct. If multiple of such designs can be installed in the regions which receives adequate sunshine, it can meet the electrical power needs of almost thousands of villages.